Cell Reports
Physical Science

CellPress
OPEN ACCESS

Article

Heterogeneity-driven collective-motion patterns of active gels

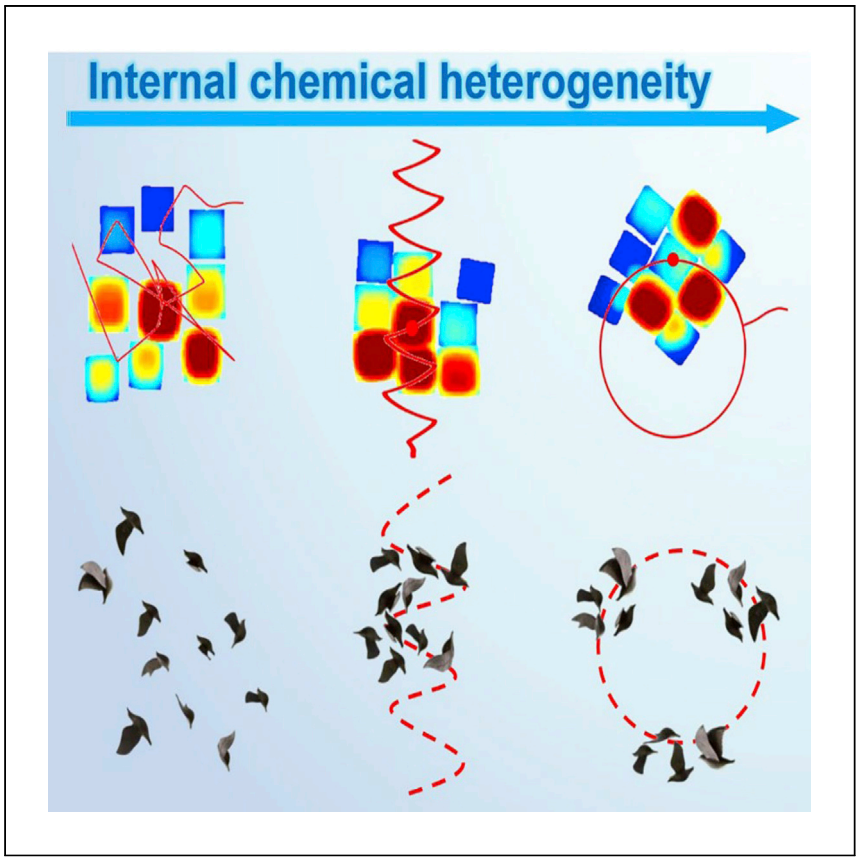

The generation of spontaneous collective-motion patterns in active groups, such as bird flocks, is a fascinating process. Teng et al. use a chemical model to explore the role of internal heterogeneity, i.e., the existence of a small number of "leaders," in generating and switching between such patterns, including irregular uncoordinated motion and coordinated swing-forward and circular motions.

Rui Teng, Qingyu Gao, Ling Yuan, Lin Ren, Jing Wang, Yunjie Wang, Irving R. Epstein

gaoqy@cumt.edu.cn (Q.G.)
epstein@brandeis.edu (I.R.E.)

Highlights

The essential role of internal heterogeneity in complex collective motion

Control of transitions between collective-motion patterns in an active group

The relationship between traveling wave dynamics and group motion patterns

Teng et al., Cell Reports Physical Science 3, 100933
June 15, 2022
https://doi.org/10.1016/j.xcrp.2022.100933

Cell Reports
Physical Science

CellPress
OPEN ACCESS

Article

Heterogeneity-driven collective-motion patterns of active gels

Rui Teng,[1] Qingyu Gao,[1,4,*] Ling Yuan,[1] Lin Ren,[2] Jing Wang,[1] Yunjie Wang,[1] and Irving R. Epstein[3,*]

SUMMARY

Biological swarms produce movement patterns that enhance their viability and functionality. We investigate the importance of internal heterogeneity within a group for the generation and transformation of group movement patterns. We find that an increase in the activity difference between a pair of chemically reactive gels and the rest causes the gel group to evolve from irregular random motion to ordered periodic swing-forward and circular motions. Our results imply that internal heterogeneity within a group is a key factor in generating ordered motion patterns, such as linear or curved locomotion, and disperse or compact population distributions. Dynamical analysis of collective pattern transitions reveals that the location and level of activity of a few "leaders" act as control parameters for bifurcations of collective-motion patterns. Our results suggest a possible origin of swarm motion patterns and may also be used to tailor robot swarms to enhance flexibility and robustness.

INTRODUCTION

In active systems, from microbes to mammals, as well as artificial active matter, individuals tend to form stable groups through self-organization.[1–3] Self-organizing groups can display remarkable feats of coordination, allowing swarms to produce a variety of stable motion patterns. Examples include predatory locusts,[4] migrating white storks,[5] and cooperative transport by ants.[6] These motion patterns enable groups to show extraordinary mobility and function. What drives these behaviors? In most studies, individuals in groups have been regarded as essentially homogeneous. Collective motion is generally thought to result from the interaction between the external environment and the collective.[7–9] However, heterogeneity among individuals is universal.[10,11]

In nature, individual heterogeneity, in traits such as perceptual ability, body shape, and gender, arises from the diversity of genes, the influence of the environment, and even the pathology of individuals.[10,12] An obvious example is multiple births: although the progeny are very similar, they still differ in some aspects. At a deeper level, heterogeneity in groups, especially with regard to competitive abilities,[13] can lead to complex interactions and collective stability.[14,15] This population asymmetry is particularly evident in cell populations, where it promotes asymmetric division and population movement of cells to differentiate into tissues with different functions.[16] Such symmetry breaking is an important factor in the collective generation of directional motion patterns. In most cases, the role of the external environment is to drive the group to produce directional movement by amplifying internal differences.[17]

Moreover, individual behaviors differ from one other, which can have major adaptive consequences and extensive ecological and evolutionary significance, such as

[1]College of Chemical Engineering, China University of Mining and Technology, Xuzhou 221008, Jiangsu, P.R. China

[2]College of Chemistry and Materials Engineering, Wenzhou University, Wenzhou 325035, Zhejiang, P.R. China

[3]Department of Chemistry and Volen Center for Complex Systems, Brandeis University, Waltham, MA 02454-9110, USA

[4]Lead contact

*Correspondence: gaoqy@cumt.edu.cn (Q.G.), epstein@brandeis.edu (I.R.E.)

https://doi.org/10.1016/j.xcrp.2022.100933

emergent collective behavior and group extinction. For example, individuals with atypical characteristics can play an emergent leadership role in collective behavior.[18] Differences within a fish group determine the function and movement behavior of the group.[19] Although several authors have considered the importance of heterogeneity, there is still no unified mechanistic understanding and description of heterogeneous groups.[10] In particular, we lack the ability to explain and predict the influence of heterogeneity on collective behavior and motion. Recent studies have found that system heterogeneity can affect the synchronization mode of group oscillations and regulate the stability of oscillations,[20,21] but few studies have focused on the relationship between heterogeneity and collective-motion patterns.

A fundamental problem is understanding the transitions between collective-motion patterns originating from internal heterogeneity. Collective-motion patterns of individuals from a single species often display diversity, which enhances the adaptability of the group. For example, a flock of birds can display random flying, swinging, or milling.[22,23] Other active groups also show transformations among patterns of collective motion.[24–28] Recent studies have tended to attribute these transformations to external conditions and system asymmetry. For example, increasing the surface-to-volume ratio of the system can promote the aggregation of roaming active particles at a boundary,[26] and the motion of bacteria can be changed from rotation to oscillation by adjusting the solution viscosity.[28] We pose the following questions: is there any correlation between motion-pattern transformation and internal heterogeneity? Can pattern transformation be controlled through internal heterogeneity? Here, we provide a novel perspective on these questions. We suggest that collective motion can arise from the internal heterogeneity of the group and that movement patterns are governed by changes in heterogeneity.

In this work, we study the effects of individual differences on collective-motion patterns using a simulated group of self-oscillating Belousov-Zhabotinsky (BZ) gels that display a rich array of biomimetic behaviors, including multiple states, periodic and aperiodic oscillations (similar to cardiac and neural rhythms), and chemomechanical transduction. A single BZ gel may be regarded as an analog of an artificial animal, cell, or robot. In a sufficiently large gel, traveling pulse waves, caused by coupling between oscillatory kinetics and diffusion, generate a net-force difference between pushing and pulling as a result of swelling and shrinking at the wave front and wave back, respectively. The ensuing locomotion can produce a variety of movement patterns, such as periodic migration[29] and amoeba-like motion.[30] Active BZ gels not only generate chemical waves to drive their own motion[31,32] but also cause diffusion into the surrounding aqueous solution of the autocatalyst u produced by the reaction. The consequent exchange of the autocatalyst results in communication between the gels,[33] which can lead to chemotactic movement of a gel group, e.g., self-aggregation and self-rotation of cubic gels.[34] Similarly, entities from unicellular organisms[35] to social arthropods[36] may exhibit a form of chemotaxis in which they pursue chemical attractants released by themselves. Especially for bacteria and single-celled organisms, this self-generated "autochemotaxis" is an important means of communication. The propagation and stability of these signals determine the group behavior and motion pattern of these organisms.[37,38]

The behavior of a gel group can be used to model such phenomena and their underlying mechanistic origin. Here, we employ a system consisting of nine active BZ gels to study the effect of internal heterogeneity on collective-motion patterns. Three distinct patterns are obtained by varying the internal heterogeneity. By increasing the activity of two gels in the group, which we refer to as the "leaders," i.e., raising their oscillatory

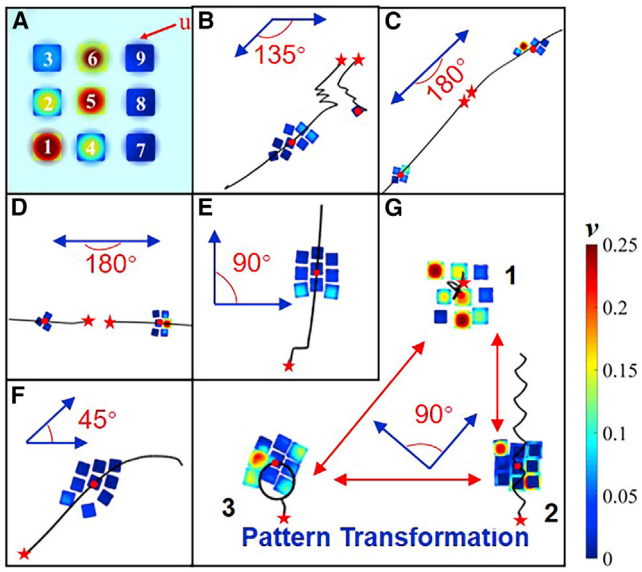

Figure 1. Motion patterns of gel populations with two leaders

(A) Initial position of gels. The gels are numbered from 1 to 9.

(B) Gels 1 and 8 as leaders.

(C) Gels 1 and 9 as leaders.

(D) Gels 2 and 8 as leaders.

(E) Gels 6 and 8 as leaders.

(F) Gels 8 and 9 as leaders.

(G) Gels 3 and 9 as leaders.

Red dots represent the center of mass of a group or the center of mass of each part of a divided group. In (B)–(F), $\Delta\varepsilon$ is set to 0.0063. In (G), $\Delta\varepsilon$ for patterns 1, 2, and 3 is set to 0.0007, 00056, and 0.0098, respectively. The red pentagram represents the starting point of the black center of mass trajectories. Angles shown have vertex at the center of the group (gel 5) and rays pointing toward the leaders. Color bar shows concentration of v in the gel. In (A), the u marked by the red arrow shows the autocatalyst concentration outside the gel.

frequency above that of the other gels in the group, we obtain irregular, swing-forward, and circular motions. We emphasize that the patterns of collective motion in our study arise from the heterogeneity within the group in a uniform external environment. From a fundamental point of view, our research can shed light on the far-from-equilibrium chemical kinetics underlying the adaptability and collective motion of active matter. It can help us to better control groups of active components to enhance their flexibility and robustness, e.g., in designing functional soft robots.

RESULTS

Effect of the number and position of heterogeneous individuals on motion patterns

Our two-dimensional system consists of nine BZ gels, each 15 × 15 units (0.06 × 0.06 cm), at the center of a 500 × 500 unit box. More details are given in materials and methods. We number our nine simulated gels as shown in Figure 1A. In all our simulations, the initial arrangement of gels is the same. Each gel is simulated using the modified Yashin-Balazs model[39–42] described in Note S1. Heterogeneity within the group is achieved by assigning different values of the model activity parameter ε_L to different gels.

In our simulations, all parameters except ε_L, which we take as a measure of the heterogeneity, are fixed, and most gels are assigned the value $\varepsilon_0 = 0.07$. Leaders are

created by setting $\varepsilon_L = \varepsilon_0 + \Delta\varepsilon$ for one or two gels in the group. Depending on the activity difference, $\Delta\varepsilon$, gel groups may exhibit different motion patterns because the frequency of chemical oscillation increases with the activity, as shown in Figure S1. We note the sharp increase in the average frequency of the diffusively coupled group at about $\Delta\varepsilon = 0.007$, in contrast with the smooth increase for an individual gel. The parameter ε measures the ratio of timescales between the fast activator/autocatalyst, *u*, ($HBrO_2$), and the slow inhibitor/oxidized catalyst, *v*, (Ru(III)), which oscillate in phase. The value of $\Delta\varepsilon$ controls the structure and propagation of the chemical waves, since the highest frequency determines the direction of wave motion. High and low *v* concentrations cause individuals in the gel group to swell and shrink at the wave front and wave back, leading to the push and the pull, respectively. The resultant net force caused by the chemical waves drives the movement of the gel group opposite to direction of wave propagation, i.e., retrograde-wave locomotion.[42]

We considered all unique cases with one or two leaders. Due to the symmetry of the gel cluster, there are three possibilities with one leader: [(1,3,7,9), (2,4,6,8), and (5)]. When the leader is placed at the outer edge of the group, the group moves in a straight line. If the more active gel is located at the central position 5, the group cannot produce directional motion. The results of these three cases are shown in Video S1. There are eight independent possibilities with two leaders: e.g., (gels 1 and 8: 8 symmetry-equivalent cases, gels 1 and 9: 2 cases, gels 2 and 8: 2 cases, gels 3 and 9: 4 cases, gels 5 and 8: 4 cases, gels 5 and 9: 4 cases, gels 6 and 8: 4 cases, and gels 8 and 9: 8 cases). When the leaders are chosen as (5,8) or (5,9), the results are similar to those found by setting one leader at the side of group, as shown in Video S2.

Here, we show the most interesting movement patterns when there are two leaders. As seen in Figures 1B–1D, when the two leaders are (1,8), (1,9), or (2,8) and the initial angle between the two leaders and the group center (direction angle) is greater than 90° (Video S3), the group splits into two subgroups. In the other cases, the group remains united. As shown in Figures 1E and 1F, when the leaders are (6,8) (direction angle 90°) or (8,9) (direction angle 45°), the gel group traces a curvilinear path, as shown in Video S4. The most striking behavior arises when gels 3 and 9 (i.e., adjacent corners, direction angle 90°) are the leaders. The group then displays a sequence of motion patterns (Figure 1G) as we increase $\Delta\varepsilon$. The transitions between these modes and their origin constitute the focus of this paper.

Transition between collective-motion modes

In contrast to previous studies, in which environmental-interaction parameters were varied,[28] we use the difference in activity within the group as the control parameter, which we believe provides a better understanding of the key role of internal dynamics in group movement. Here, we focus on the transitions between motion modes caused by increasing the activity difference between the leader gels 3 and 9 and the other gels.

When $\Delta\varepsilon$ is small, i.e., $\leq$0.0014, we observe disordered, irregular motion, as shown in Figure 2A,[22,23] with $\Delta\varepsilon = 0.0007$. When the activity difference is greater, $\Delta\varepsilon$ = 0.0014–0.0070, orderly collective-motion patterns emerge, in which the group generates a swing-forward-motion pattern. We show a typical trajectory with $\Delta\varepsilon$ = 0.0056 in Figure 2B. The gels swing back and forth in the x direction and move upward in the y direction. When the gel group approaches the upper boundary of the box, this movement ceases as the result of the influence of the boundary. Finally,

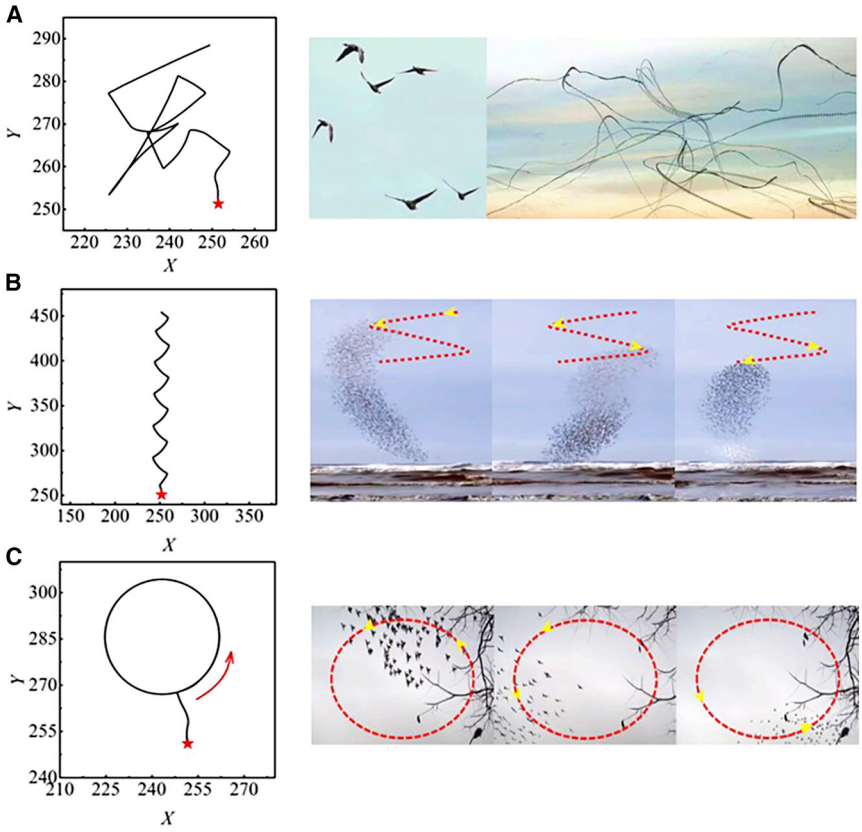

Figure 2. Collective motion of gel group and bird flock

(A) Left: irregular motion at $\Delta\varepsilon = 0.0007$. Right: irregular motion in flock of birds (https://plainmagazine.com/hypnotizing-look-flight-patterns-birds-xavi-bou/).

(B) Left: swing-forward motion at $\Delta\varepsilon = 0.0056$. Right: swing-forward motion in flock of birds (https://gfycat.com/pettyspectacularеidolonhelvum).[22]

(C) Left: circular motion at $\Delta\varepsilon = 0.0098$. Right: circular motion in flock of birds (https://www.youtube.com/watch?v=8uETLpdbh4k).[23]

The red star represents the gel position of the starting point. The arrow indicates the direction of rotation of the gel group in the circular motion.

when the activity difference exceeds 0.007, the group first makes a small turn and then undergoes circular motion, which is shown in Figure 2C at $\Delta\varepsilon = 0.0098$. Once the gel group begins to circle, the trajectories of successive cycles coincide nearly perfectly. Similar motion modes can be observed in nature, e.g., in the movement of flocks of birds, as seen in the righthand column of Figure 2.

Kinematic quantities for measuring the gels' collective motion

We introduce the dispersion parameter, τ, to characterize changes in the spatial distribution of the gel group, which is defined as the mean square deviation of the center of each gel from the group center of mass:

$$\tau = \frac{\sqrt{\sum_{I=1}^{N}(|\vec{r_T} - \vec{r_I}|)^2}}{N}, \qquad \text{(Equation 1)}$$

where $\vec{r_T}$, $\vec{r_I}$, and N (= 9 for our simulations) are the group center, the center of each gel and the number of gels, respectively.

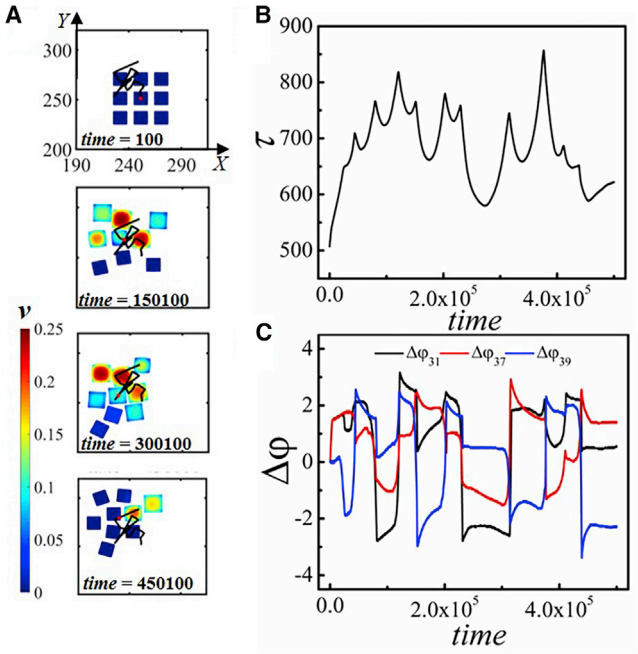

Figure 3. Irregular motion at $\Delta\varepsilon = 0.0007$

(A) Group trajectories. Red dot represents the center of mass of the gel group, whose trajectory is shown by the black line.

(B) Dispersion parameter versus time.

(C) Phase differences versus time (see Video S5).

The gels communicate through the leaching and diffusion of the autocatalyst, u, resulting in the propagation of chemical waves between gels, which causes the movement of the gels. We define the phase of oscillations, φ_i, and the phase difference, $\Delta\varphi_{ij}$, as

$$\varphi_i(t) = \frac{2\pi(t - t_k)}{(t_{k+1} - t_k)} \quad (t_k < t < t_{k+1}), \qquad \text{(Equation 2)}$$

$$\Delta\varphi_{ij} = \varphi_i - \varphi_j \qquad \text{(Equation 3)}$$

where t_k is the peak time of the kth chemical oscillation in gel i, and i or j is the index number of the gel. Comparing the phase differences, $\Delta\varphi_{ij}$, we can obtain the direction of chemical-wave propagation. If the phase difference $\Delta\varphi_{ij}$ is positive and less than 2π, gel i oscillates before gel j, and the propagation direction is i to j.

Irregular motion

To understand the irregular motion, we examine the sequence of loci of the gel group in Figure 3A (Video S5). The group is loose and moves irregularly, with an erratic trajectory for the central locus of the group. No cooperativity is evident. The behavior of the dispersion parameter (Equation 1) during this motion is shown in Figure 3B. It first rises rapidly with time and then fluctuates, confirming that that the gel population is irregular and loose. Further insight is provided by the phase differences in Figure 3C. Gels 1, 3, 7, and 9 are initially located at the four corners of the group, and chemical waves are most likely to arise at these positions. Therefore, we consider the phase differences obtained from the local oscillations at the central points of these four gels to investigate the propagation of chemical waves in the group. The phase differences $\Delta\varphi_{31}$, $\Delta\varphi_{37}$, and $\Delta\varphi_{39}$ vary irregularly between 3 and 4, implying that there is no stable chemical

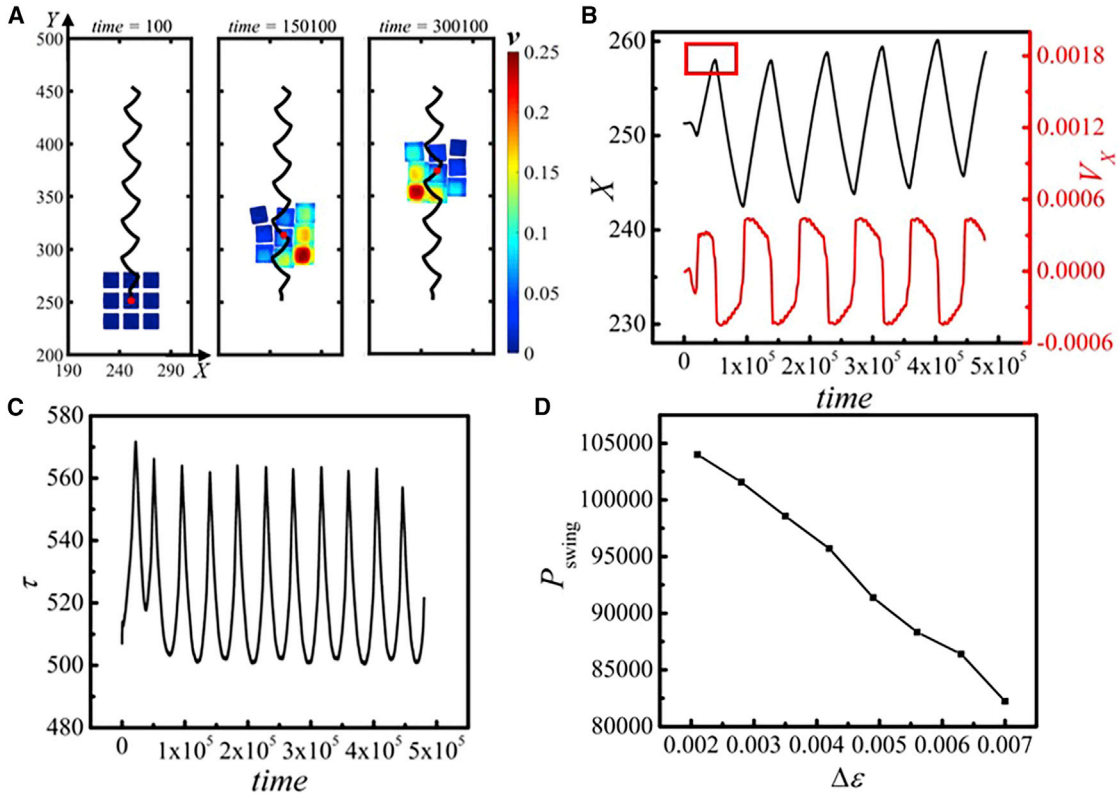

Figure 4. Swing-forward collective motion and kinematics of gel group at $\Delta\varepsilon$ = 0.0056

(A) Snapshots of swing-forward collective motion.

(B) Periodic oscillations of the central locus (black line) and group velocity (red line) in the x direction.

(C) Oscillations of dispersion parameter for group.

(D) Effect of $\Delta\varepsilon$ on the swing period (see Video S6).

wave in the gel group and that the propagation of chemical waves is disordered. Because the difference in activity is small, the initial frequency of gels 3 and 9 is close to that of the other gels. Therefore, the chemical waves emitted by gels 3 and 9 have not yet reached the end of the group when the other gels begin to initiate new waves, preventing the chemical waves from spreading steadily.

Swing-forward motion

Next, we analyze the evolution of the group in swing-forward motion, as shown in Video S6. Snapshots of the gel group at several times are shown in Figure 4A. The motion is driven by pulse waves, as shown in Video S7, in which the group moves to the right when the wave propagates to the left. During swing-forward motion, the three gels in a column swing in unison, like cilia. During the swing process, the center of the gel group moves periodically. We note that ciliary movement has been extensively studied[43] when the swing motion requires magnetic or other external driving forces.

The mass center of the gel group oscillates periodically in the x direction as does the velocity of the group center (Figure 4B). The oscillations appear to be asymmetric, and the velocity oscillations have a pronounced relaxation waveform. These oscillations in velocity drive the group back and forth in the x direction by about 15 units and upward in the y direction by about twice that distance during each cycle, with

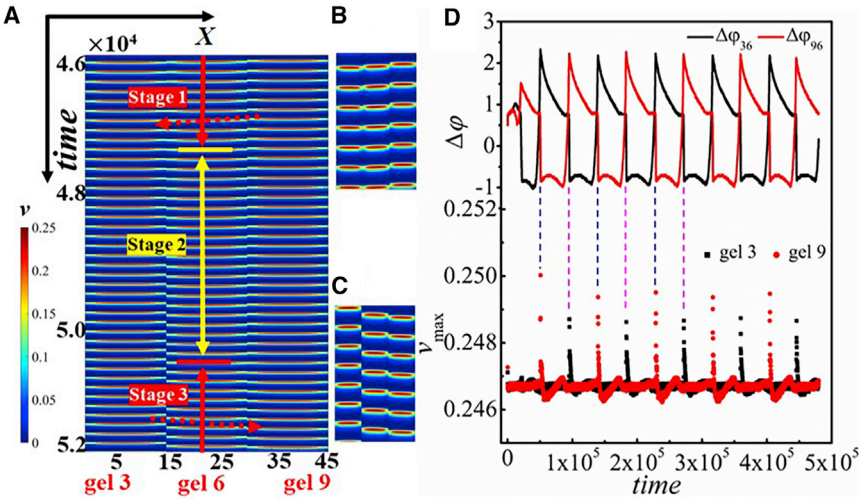

Figure 5. Kinematics of swing-forward collective motion at $\Delta\varepsilon = 0.0056$

(A) Spatiotemporal pattern of chemical-wave propagation along the midline of gels 3, 6, and 9.

(B and C) Enlargements of stages 2 and 1, respectively.

(D) Phase differences and variation of v_{max} with time in gels 3 and 9.

a period of P_{swing} = 88,333.4. The dispersion parameter, τ, (Figure 4C), varies with a period, P_τ = 44166.2, half that of a full swing. The period, P_{swing}, of the swing motion decreases gradually with the activity difference, $\Delta\varepsilon$ (Figure 4D), which provides a means to control this behavior.

To analyze the dynamic origin of the swing-forward motion, we consider the chemical-wave-propagation process in the gel group. During the motion, the relative positions of the gels remain as in Figure 1A, though the distance between gels changes. As seen in Video S6, the relative horizontal position of gels 3, 6, and 9 is nearly constant during the movement, which allows us to plot the horizontal spatiotemporal concentration pattern of oxidized catalyst, v. This spatiotemporal pattern enables us to visualize the propagation of chemical waves in order to analyze the swing motion. At t = 46,000–52,000 (red box in Figure 4B), the group is at a turning stage. In Figure 5A, we show a series of snapshots through the centers of gels 3, 6, and 9, omitting the intervening solution. We see propagation of a chemical wave opposite to the direction of motion of the gel group. In stage 1 of the spatiotemporal map, the chemical wave propagates toward gel 3, where its propagation direction is indicated by the dotted arrow (Figure 5A) and seen in an enlarged view (Figure 5B), while the group moves toward more positive x, i.e., toward gel 9. At the end of stage 1, the chemical wave passes through a transitional period, stage 2, during which the oscillations in gels 3 and 9 precede those of gel 6, so that no stable unidirectional wave is formed. In stage 3, the chemical wave completes the reversal of its direction of propagation: it now starts from gel 3 and moves through gel 6 to gel 9 (Figure 5A), as seen in the enlarged view in Figure 5C. Simultaneously, the movement direction of the group reverses, and it begins to move in the negative x direction. The results clearly show that the motion during the swing is retrograde-wave locomotion,[42] i.e., the gel moves in the opposite direction to the wave propagation. We conclude that the swing motion in the x direction is due to the spontaneous reversal of the direction of wave propagation in the group. In Figure S2, we show a similar analysis in the vertical direction, along the center line of gels 1, 2, and 3. Because the leaders reside on the upper edge of the group, the chemical wave always propagates in the negative y

direction, causing the group to move in the positive y direction via retrograde-wave locomotion.

The spontaneous change in the direction of chemical-wave propagation leads to the swing motion of the group. To understand the origin of this change, we examine the time evolution of the phase differences and oscillatory maxima, v_{max}, (v_{max} in each gel is the maximum over one cycle of oscillation) within the gel group. As shown in the supplemental information, analysis of the transmission of autocatalyst through the solution (Figure S3) demonstrates that we can ignore the influence of the box boundary on inter-gel communication. We use the phase difference to describe the motion process (Figure 5D, top half). Because gel 6 is located between the two leaders, gels 3 and 9, the swing movement of these three gels is the most obvious. Therefore, we take gel 6 as the representative of the follower gels to study the influence of gels 3 and 9 on the group movement. $\Delta\varphi_{36}$ and $\Delta\varphi_{96}$ vary periodically, increasing nearly vertically to positive then decreasing slowly, followed by a sharp decrease to negative after a very short plateau. The rapid rise and fall are caused by the wave reversal in stage 2 (Figure 5A). The slow decline and the plateau stage, since the phase difference is positive, correspond to gel 6 following this leader movement. The alternation of the two peaks indicates that gel 6 spontaneously changes its direction of motion, resulting from reversal of the wave propagation. Wave reversal stems from periodic, anti-phase oscillations in phase difference between the two pairs of gels (Figure 5D). The concentration extremum of the oxidized metal catalyst, v_{max}, at the center point of gels 3 and 9 is shown in the bottom half of Figure 5D. We see that the v_{max} jump in leader gels 3 and 9 alternates, which corresponds to the reversal of wave propagation. The periodic oscillatory dynamics of v_{max} in the leader gels produces wave-reversal-driven periodic swings of the gel along the transverse direction, and wave propagation along the longitudinal direction drives the unidirectional upward motion, resulting in the observed swing-forward motion.

Formation and dynamics of circular motion

During circular motion, the whole gel population is tightly aggregated, and the shape of the gel array remains nearly constant, as shown in Video S8. The transition from swing to circular motion results from a change in the type of chemical wave. Unlike swing motion, which is driven by pulse waves, circular motion arises from spiral waves in the gel group, generated by the same mechanism as spiral waves in a single gel.[44] Before the initiation of circular motion, the group swings to the left a short distance, with gel 3 as the leader (a spatiotemporal sequence is shown in Figure 6A). In the course of this swing, the excited pulse wave from gel 9 is blocked by the relatively large gap between gels 9 and 6, and the wave cannot propagate to gel 6, which leads to the waves curling to form a spiral (Figure 6B; Video S9), causing the group to undergo circular motion, as shown in Figure 6C. The corresponding evolution of v_{max} is shown in Figure 6D. At about t = 30,336 (the transition time), the leftward motion stops, and the gel enters the stage of dynamic change. When the gel turns back to the right after the v_{max} of gel 3 jumps (Figure 6D, black dot in the red dashed box), it enters a new process, during which a wave starts from gel 9 and finally forms a spiral wave. At the same time, the other gels in the group also experience a decrease in v_{max} (red dot in Figure 6D). The time course of the dispersion parameter for spiral-wave formation is highlighted in the red dotted box in Figure 6E, where the gel dispersity at the transition point is much greater than that in swing-forward motion, resulting in obvious spatial heterogeneity at t = 30,050 in Figure 6A. Such spatial heterogeneity is known to lead to the generation of spiral waves.[45,46]

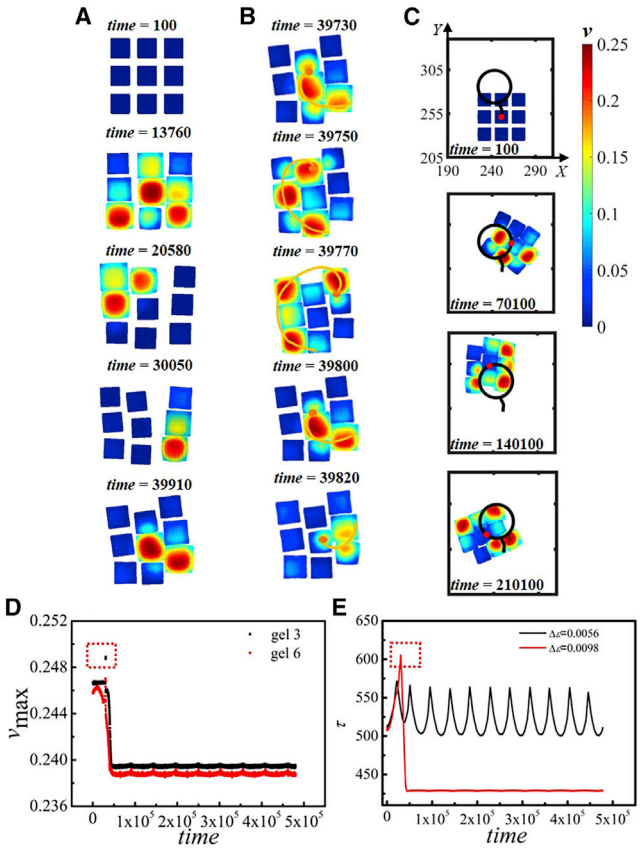

Figure 6. Spiral-wave formation and circular motion of gel group at $\Delta\varepsilon = 0.0098$

(A) Snapshots of gel group before spiral-wave production.

(B) Snapshots of one cycle of spiral waves in gel group.

(C) Group trajectories of circular motion.

(D) Time evolution of oscillatory maximum v_{max}.

(E) Time evolution of dispersion parameter for swing-forward motion and circular motion (Videos S8 and S9).

Bifurcation of collective-movement patterns

As we have seen, the collective motion changes with the activity difference $\Delta\varepsilon$. In essence, these changes are caused by the dynamic evolution of the chemical oscillations in the active gels. Here, we study the variation in oscillatory maximum, v_{max}, and the dispersion parameter, τ, of the three motion patterns after they have stabilized (t > 150,000). Figure 7A shows v_{max} for oscillations at the center of gel 3 as a function of the activity difference, $\Delta\varepsilon$, which, because of the synchronous system dynamics, provides insight into the dynamics of the entire gel group. When the gel group exhibits irregular movement, v_{max} exhibits irregular, apparently random, fluctuations (black time series in insert), which are caused by initial noise and group interaction. In contrast, in the swing-forward motion, v_{max} shows regular periodic oscillations (red time series in insert). When the activity difference rises above 0.0070, the v_{max} decreases sharply and then remains at a steady low value as $\Delta\varepsilon$ is further increased. The collective order parameter τ also undergoes sharp changes when the mode of group motion switches with increasing activity difference (Figure 7B). The parallel behavior of these two kinetic parameters in response to the changes induced by activity difference highlights the close relationship between the local dynamics, the spatial dispersion, and collective-motion patterns.

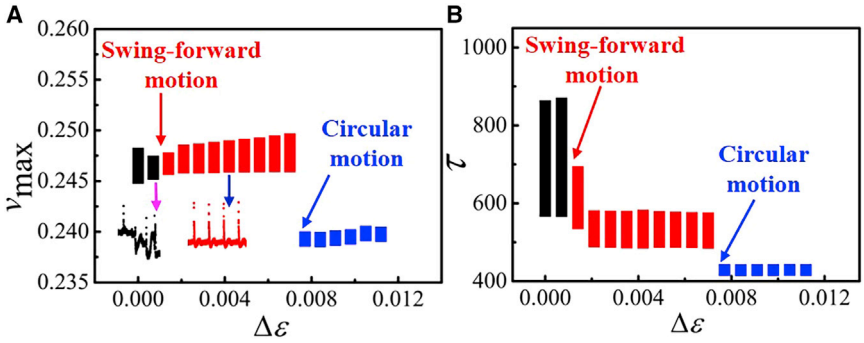

Figure 7. Effect of activity difference on chemical oscillatory dynamics and collective order parameter

(A) Variation in extremum of oxidized catalyst v_{max} for gel 3.

(B) Variation in collective dispersion parameter τ.

Black, red, and blue represent irregular, swing-forward, and circular motions, respectively. Inserts in (A) show time series of v_{max} at the values of $\Delta\varepsilon$ indicated by the arrows.

Bifurcations of the chemical-wave-propagation process induced by the activity difference produce qualitative changes in the spatial structure of the group and in its mode of motion.

DISCUSSION

The multifold behavior of active-matter collective motion is a thought-provoking process that originates from the interaction among individuals, especially the complex interplay between the heterogeneity of individuals and the homogenizing effect of diffusion. This competition between heterogeneity and homogenization leads to a variety of dynamic states, producing different collective-motion patterns. Unidirectional motion occurs in a gel population with a single heterogeneous individual. However, with two leaders, there are more possibilities. When the initial angle between the lines connecting the two leaders and the group center exceeds 90°, multiple independent waves are initiated, as shown in Figures 1B–1D, causing the gel group to separate into two parts. When this angle is less than or equal to 90°, the group remains together and exhibits various modes of collective motion. Our research also demonstrates the plasticity of collective-motion patterns: three types of patterns emerge on adjusting the activity difference when the two leaders are gels 3 and 9: irregular, swing-forward, and circular motions. It should be emphasized that heterogeneity lies at the origin of this collective motion. The coupling between BZ oscillations and autocatalyst diffusion gives rise to waves propagating between gels. The net force at each gel, driven by the chemical waves, points in the direction opposite that of the wave propagation, resulting in synchronous retrograde-wave locomotion of the individual gels. The specific synchronization mode is determined by the number and type of the chemical waves. Our study reveals the internal mechanism of various collective-motion patterns and suggests approaches to their control and robustness, pointing toward a vision for the design of intelligent swarm robots.[47]

Here, we have studied the effects on collective motion of one and two heterogeneous individuals in an array of nine active gels. Activity differences in an experiment can be realized by, for example, employing different catalyst concentrations or types (e.g., ruthenium, ferroin, etc.) in different gels. Changing the ratio of monomer and crosslinking agent in gel synthesis can also change the activity of the gel, affecting the coupling constant χ^* and the cross-link density c_0 in the model. In the real world, groups contain more individuals, and the distribution of heterogeneous individuals is more complex.

Therefore, more in-depth research is needed in the future. For example, using heterogeneous individuals with multiple activity differences, expanding the size of the group, and increasing the number of heterogeneous individuals also need to be considered, which will help us understand more complex functions of artificial and natural active groups.

EXPERIMENTAL PROCEDURES

Resource availability

Lead contact

Further information and requests for resources should be directed to and will be fulfilled by the lead contact, Qingyu Gao (gaoqy@cumt.edu.cn).

Materials availability

This study did not generate new unique materials.

Data and code availability

All data needed to support the conclusions of this manuscript are included in the main text or supplemental information.

Additional data and code are available from the lead contact, Qingyu Gao, upon reasonable request.

Materials and methods

Our model is derived from variants of the gel elastic lattice model (gLSM).[39–42] The governing partial differential equations (PDEs) and computational details are given in Note S1: Model and method. The nine BZ gels (each 15 × 15 units) are placed in the center of a two-dimensional 500 × 500 unit box with 3 units separating adjacent gels. The arrangement of the gels is shown in Figure 1A. The boundary of the box has a fixed concentration of autocatalyst, $u = 0$. The gels communicate with each other through u, which is produced in the gel via the BZ reaction, diffusing and decomposing in the solution according to Equation S3. The choice of the gels' heterogeneity, ε, is described in the Results.

SUPPLEMENTAL INFORMATION

Supplemental information can be found online at https://doi.org/10.1016/j.xcrp.2022.100933.

ACKNOWLEDGMENTS

This work was supported by the National Natural Science Foundation of China (grant nos. 22120102001 and 21972165), the Natural Science Foundation of Jiangsu Province (grant no. BK20211242), and grant CHE-1856484 from the US National Science Foundation. We are grateful to the Advanced Analysis and Computation Center of CUMT for the award of CPU hours to accomplish the computations in this paper.

AUTHOR CONTRIBUTIONS

R.T., Q.G., and I.R.E. designed research; R.T., Q.G., Y.L., L.R., J.W., Y.W., and I.R.E. performed research; L.R., R.T., Q.G., and I.R.E. analyzed data; and R.T., Q.G., and I.R.E. wrote the paper.

DECLARATION OF INTERESTS

The authors declare no competing financial interest.

Received: March 3, 2022
Revised: April 18, 2022
Accepted: May 18, 2022
Published: June 8, 2022

REFERENCES

1. Bechinger, C., Di Leonardo, R., Löwen, H., Reichhardt, C., Volpe, G., and Volpe, G. (2016). Active particles in complex and crowded environments. Rev. Mod. Phys. *88*, 045006. https://doi.org/10.1103/revmodphys.88.045006.

2. Gompper, G., Winkler, R.G., Speck, T., Solon, A., Nardini, C., Peruani, F., Löwen, H., Golestanian, R., Kaupp, U.B., Alvarez, L., et al. (2020). The 2020 motile active matter roadmap. J Phys. Condens. Mat. *32*, 193001. https://doi.org/10.1088/1361-648X/ab6348.

3. Shaebani, M.R., Wysocki, A., Winkler, R.G., Gompper, G., and Rieger, H. (2020). Computational models for active matter. Nat. Rev. Phys. *2*, 181–199. https://doi.org/10.1038/s42254-020-0152-1.

4. Ariel, G., and Ayali, A. (2015). Locust collective motion and its modeling. PLoS Comput. Biol. *11*. e1004522. https://doi.org/10.1371/journal.pcbi.1004522.

5. Flack, A., Nagy, M., Fiedler, W., Couzin, I.D., and Wikelski, M. (2018). From local collective behavior to global migratory patterns in white storks. Science *360*, 911–914. https://doi.org/10.1126/science.aap7781.

6. Feinerman, O., Pinkoviezky, I., Gelblum, A., Fonio, E., and Gov, N.S. (2018). The physics of cooperative transport in groups of ants. Nat. Phys. *14*, 683–693. https://doi.org/10.1038/s41567-018-0107-y.

7. Sosna, M.M.G., Twomey, C.R., Bak-Coleman, J., Poel, W., Daniels, B.C., Romanczuk, P., and Couzin, I.D. (2019). Individual and collective encoding of risk in animal groups. Proc. Natl. Acad. Sci. U S A *116*, 20556–20561. https://doi.org/10.1073/pnas.1905585116.

8. Calabrese, J.M., Fleming, C.H., Fagan, W.F., Rimmler, M., Kaczensky, P., Bewick, S., and Leimgruber, P. (2018). Disentangling social interactions and environmental drivers in multi-individual wildlife tracking data. Philos. Trans. R. Soc. B. *373*, 20170007. https://doi.org/10.1098/rstb.2017.0007.

9. Schaerf, T.M., Dillingham, P.W., and Ward, A.J.W. (2017). The effects of external cues on individual and collective behavior of shoaling fish. Sci. Adv. *3*. e1603201. https://doi.org/10.1126/sciadv.1603201.

10. Jolles, J.W., King, A.J., and Killen, S.S. (2020). The role of individual heterogeneity in collective animal behaviour. Trends Ecol. Evol. *35*, 278–291. https://doi.org/10.1016/j.tree.2019.11.001.

11. Salek, M.M., Carrara, F., Fernandez, V., Guasto, J.S., and Stocker, R. (2019). Bacterial chemotaxis in a microfluidic T-maze reveals strong phenotypic heterogeneity in chemotactic sensitivity. Nat. Commun. *10*, 1877. https://doi.org/10.1038/s41467-019-09521-2.

12. Gaston, K.J., and Spicer, J.I. (2013). Biodiversity: An Introduction (John Wiley and Sons).

13. Bruce, A.I., Czaczkes, T.J., and Burd, M. (2017). Tall trails: ants resolve an asymmetry of information and capacity in collective maintenance of infrastructure. Anim. Behav. *127*, 179–185. https://doi.org/10.1016/j.anbehav.2017.03.018.

14. Karamched, B., Stickler, M., Ott, W., Lindner, B., Kilpatrick, Z.P., and Josić, K. (2020). Heterogeneity improves speed and accuracy in social networks. Phys. Rev. Lett. *125*, 218302. https://doi.org/10.1103/physrevlett.125.218302.

15. Miguel, M.C., Parley, J.T., and Pastor-Satorras, R. (2018). Effects of heterogeneous social interactions on flocking dynamics. Phys. Rev. Lett. *120*, 068303. https://doi.org/10.1103/physrevlett.120.068303.

16. Costa, G., Harrington, K.I., Lovegrove, H.E., Page, D.J., Chakravartula, S., Bentley, K., and Herbert, S.P. (2016). Asymmetric division coordinates collective cell migration in angiogenesis. Nat. Cell Biol. *18*, 1292–1301. https://doi.org/10.1038/ncb3443.

17. Webster, M.M., Whalen, A., and Laland, K.N. (2017). Fish pool their experience to solve problems collectively. Nat. Ecol. Evol. *1*, 135. https://doi.org/10.1038/s41559-017-0135.

18. Mann, R.P. (2020). Collective decision-making by rational agents with differing preferences. Proc. Natl. Acad. Sci. U S A *117*, 10388–10396. https://doi.org/10.1073/pnas.2000840117.

19. Jolles, J.W., Boogert, N.J., Sridhar, V.H., Couzin, I.D., and Manica, A. (2017). Consistent individual differences drive collective behavior and group functioning of schooling fish. Curr. Biol. *27*, 2862–2868.e7. https://doi.org/10.1016/j.cub.2017.08.004.

20. Zhang, Y., Ocampo-Espindola, J.L., Kiss, I.Z., and Motter, A.E. (2021). Random heterogeneity outperforms design in network synchronization. Proc. Natl. Acad. Sci. U S A *118*. e2024299118. https://doi.org/10.1073/pnas.2024299118.

21. Xu, C., and Zheng, Z. (2019). Bifurcation of the collective oscillatory state in phase oscillators with heterogeneity coupling. Nonlinear Dynam. *98*, 2365–2373. https://doi.org/10.1007/s11071-019-05336-4.

22. Hemelrijk, C.K., van Zuidam, L., and Hildenbrandt, H. (2015). What underlies waves of agitation in starling flocks. Behav. Eco. Sociobiol. *69*, 755–764. https://doi.org/10.1007/s00265-015-1891-3.

23. Chen, D., Xu, B., Zhu, T., Zhou, T., and Zhang, H.T. (2017). Anisotropic interaction rules in circular motions of pigeon flocks: an empirical study based on sparse Bayesian learning. Phys. Rev. E. *96*, 022411. https://doi.org/10.1103/physreve.96.022411.

24. Mueller, R., Yeomans, J.M., and Doostmohammadi, A. (2019). Emergence of active nematic behavior in monolayers of isotropic cells. Phys. Rev. Lett. *122*, 048004. https://doi.org/10.1103/physrevlett.122.048004.

25. Franks, N.R., Worley, A., Grant, K.A.J., Gorman, A.R., Vizard, V., Plackett, H., Doran, C., Gamble, M.L., and Stumpe, M.C. (2016). Social behaviour and collective motion in plant-animal worms. Proc. Biol. Sci. *283*, 20152946. https://doi.org/10.1098/rspb.2015.2946.

26. Deblais, A., Barois, T., Guerin, T., Delville, P.H., Vaudaine, R., Lintuvuori, J.S., Boudet, J., and Baret, J. (2018). Boundaries control collective dynamics of inertial self-propelled robots. Phys. Rev. Lett. *120*, 188002. https://doi.org/10.1103/physrevlett.120.188002.

27. Huang, Z.F., Menzel, A.M., and Löwen, H. (2020). Dynamical crystallites of active chiral particles. Phys. Rev. Lett. *125*, 218002. https://doi.org/10.1103/physrevlett.125.218002.

28. Liu, S., Shankar, S., Marchetti, M.C., and Wu, Y. (2021). Viscoelastic control of spatiotemporal order in bacterial active matter. Nature *590*, 80–84. https://doi.org/10.1038/s41586-020-03168-6.

29. Ren, L., Wang, M., Pan, C., Gao, Q., Liu, Y., and Epstein, I.R. (2017). Autonomous reciprocating migration of an active material. Proc. Natl. Acad. Sci. U S A *114*, 8704–8709. https://doi.org/10.1073/pnas.1704094114.

30. Onoda, M., Ueki, T., Tamate, R., Shibayama, M., and Yoshida, R. (2017). Amoeba-like self-oscillating polymeric fluids with autonomous sol-gel transition. Nat. Commun. *8*, 15862. https://doi.org/10.1038/ncomms15862.

31. Yoshida, R., Takahashi, T., Yamaguchi, T., and Ichijo, H. (1996). Self-oscillating gel. J. Am. Chem. Soc. *118*, 5134–5135. https://doi.org/10.1021/ja9602511.

32. Lu, X., Ren, L., Gao, Q., Zhao, Y., Wang, S., Yang, J., and Epstein, I.R. (2013). Photophobic and phototropic movement of a self-oscillating

gel. Chem. Commun. *49*, 7690–7692. https://doi.org/10.1039/c3cc44480e.

33. Yoshida, R., Tanaka, M., Onodera, S., Yamaguchi, T., and Kokufuta, E. (2000). In-phase synchronization of chemical and mechanical oscillations in self-oscillating gels. J. Phys. Chem. A. *104*, 7549–7555. https://doi.org/10.1021/jp0011600.

34. Dayal, P., Kuksenok, O., and Balazs, A.C. (2013). Reconfigurable assemblies of active, autochemotactic gels. Proc. Natl. Acad. Sci. U S A *110*, 431–436. https://doi.org/10.1073/pnas.1213432110.

35. King, J.S., and Insall, R.H. (2009). Chemotaxis: finding the way forward with Dictyostelium. Trends Cell Biol. *19*, 523–530. https://doi.org/10.1016/j.tcb.2009.07.004.

36. Jackson, B.D., and Morgan, E.D. (1993). Insect chemical communication: pheromones and exocrine glands of ants. Chemoecology *4*, 125–144. https://doi.org/10.1007/bf01256548.

37. Eckstein, T.F., Vidal-Henriquez, E., Bae, A.J., and Gholami, A. (2020). Spatial heterogeneities shape the collective behavior of signaling amoeboid cells. Sci. Signal. *13*, eaaz3975. https://doi.org/10.1126/scisignal.aaz3975.

38. Thomas, M.A., Kleist, A.B., and Volkman, B.F. (2018). Decoding the chemotactic signal. J. Leukoc. Biol. *104*, 359–374. https://doi.org/10.1002/jlb.1mr0218-044.

39. Yashin, V.V., and Balazs, A.C. (2006). Modeling polymer gels exhibiting self-oscillations due to the Belousov– Zhabotinsky reaction. Macromolecules *39*, 2024–2026. https://doi.org/10.1021/ma052622g.

40. Yashin, V.V., and Balazs, A.C. (2007). Theoretical and computational modeling of self-oscillating polymer gels. J. Chem. Phys. *126*, 124707. https://doi.org/10.1063/1.2672951.

41. Kuksenok, O., Yashin, V.V., and Balazs, A.C. (2008). Three-dimensional model for chemoresponsive polymer gels undergoing the Belousov-Zhabotinsky reaction. Phys. Rev. E. *78*, 041406. https://doi.org/10.1103/physreve.78.041406.

42. Ren, L., Yuan, L., Gao, Q., Teng, R., Wang, J., and Epstein, I.R. (2020). Chemomechanical origin of directed locomotion driven by internal chemical signals. Sci. Adv. *6*. eaaz9125. https://doi.org/10.1126/sciadv.aaz9125.

43. Sanchez, T., Welch, D., Nicastro, D., and Dogic, Z. (2011). Cilia-like beating of active microtubule bundles. Science *333*, 456–459. https://doi.org/10.1126/science.1203963.

44. Ren, L., Wang, L., Gao, Q., Teng, R., Xu, Z., Wang, J., and Pan, C. (2020). Programmed locomotion of an active gel driven by spiral waves. Angew. Chem. Int. Edit. *132*, 7172–7178. https://doi.org/10.1002/ange.202000110.

45. El-Sherif, N., Mehra, R., Gough, W.B., and Zeiler, R.H. (1982). Ventricular activation patterns of spontaneous and induced ventricular rhythms in canine one-day-old myocardial infarction. Evidence for focal and reentrant mechanisms. Circ. Res. *51*, 152–166. https://doi.org/10.1161/01.res.51.2.152.

46. Maselko, J., and Showalter, K. (1991). Chemical waves in inhomogeneous excitable media. Phys. D: Nonlinear Phenom. *49*, 21–32. https://doi.org/10.1016/0167-2789(91)90189-g.

47. Kaspar, C., Ravoo, B.J., van der Wiel, W.G., Wegner, S.V., and Pernice, W.H.P. (2021). The rise of intelligent matter. Nature *594*, 345–355. https://doi.org/10.1038/s41586-021-03453-y.